Chapter 8
Engineering Groundwater of Bedrock Area

8.1 Concepts and Classifications of Groundwater in Bedrock Area

8.1.1 Concept of the Bedrock Groundwater

The concept about fissure water in hydrogeological literature was first introduced by former Soviet Union scholar, Г.Н. Каменский and А.Н. Семихатов. In their book named *Soviet Hydrogeology* written in 1932, the groundwater in fissure and limestone was unified to the term of "groundwater flow," which was defined as follows: it can flow along the hard rock fissures, cracks, holes, or other channels according to a certain rule and has larger flow velocity and flux and higher temperature. Based on this, the "groundwater flow" was further divided into two subclasses, "groundwater flow in fissure rocks," and "cave river in limestone areas." The groundwater in fractured rocks and in porous rocks has been distinguished, and the following scholars put forward the basic concept of fissure water and karst water according to this concept mentioned above.

8.1.2 Classification of the Bedrock Groundwater

The clear concept of fissure water in hydrogeology was formally put forward by Ф.П. Саворенский, the well-known former Soviet Union scholar, and fissure water was defined as an independent type of groundwater. In the book of *Hydrogeology* written in 1935, for the parts about classification of groundwater, Ф.П. Саворенский divided the confined water into two subcategories of fissure water and karst water. The fissure water is the groundwater that buried in the fracture fissure of geologic structure. In the hydrogeological textbook written by Ф.П. Саворенский in 1939, the classification of groundwater and basic concepts of

Y. Tang et al., *Groundwater Engineering*, Springer Natural Hazards,
DOI 10.1007/978-981-10-0669-2_8

various types of groundwater were made further correction. The groundwater was divided into five categories in this book, namely: soil water (including swamp water and perched water), phreatic water, karst water, artesian water, and vein water (fissure water). Besides the soil water, the author gave definitions for the various groundwater types as the following:

Phreatic water—the groundwater in the surface sediments and upper layer of weathering crust;

Artesian water—the groundwater in the sedimentary structure (basin);

Karst water (cavern water)—the groundwater in limestone, dolomite, and other soluble rocks;

Vein water (fissure water)—the groundwater that mainly in structural fissure.

From present point of view in evaluating the groundwater classification, the main problem is that both the hydraulic properties of aquifer (or buried characteristics of aquifer) and the medium type constitute the basis for classification. As such, the characters of groundwater types were mutual tolerance and uniqueness. For example, under certain buried conditions, karst water and fissure water can also be the phreatic water or artesian water. In addition, the definitions of some groundwater types are not scientific and rigorous. Artesian water not only exists in sedimentary basin, and fissure water not always distributes as the shape of vein and only in structural fractures. Although there are some defects in this classification discussed above, it is the first and the most comprehensive classification scheme of groundwater in the discipline history of hydrogeology. Based on Саворенский classification, the Russia and China scholars developed various classification schemes for groundwater.

Following the Саворенский classification, А.Н. Овчиников, the former Soviet Union scholar, proposed a more comprehensive and precise classification of groundwater in 1949 to overcome the defects of Саворенский classification scheme. In his book of *Common Hydrogeology* (Soviet higher school teaching material) written in 1949, according to the burial conditions, groundwater was clearly divided into three types, namely upper perched water, phreatic water, and artesian water. According to the aquifer lithology, the above three types of groundwater were further divided into two subclasses of pore water and fissure water. In the description of the subclass, the karst water belonged to fissure water. But the fissure water and karst water were as the separate chapters in this book. In other words, the groundwater was actually divided into three types of pore water, fissure water, and karst water according to the aquifer lithology. In addition, the author gave a widely accepted definition for fissure water which was the groundwater in fracture rock, such as igneous rock and sedimentary rock. This definition was obviously more comprehensive than the Саворенский classification of "fissure water is the groundwater that mainly in structural fracture."

The classification of А.Н. Овчиников has many advantages. It not only summarized the basic types of groundwater, and also reflects the two main characteristics of hydraulic properties and medium types for various types of groundwater. Thus, this classification scheme was widely accepted and used in the field of hydrogeology. Various groundwater classification schemes are basically following

the A.H. Овчиников classification, in which the classification of groundwater was divided according to the hydraulic properties and medium type.

Hydrogeologists around the world have a similar view about the groundwater classification based on hydraulic properties. The groundwater of which has a higher pressure above the aquifer was referred to as artesian water. However, this definition has some limitations and according to the establish basis of the two differential equation types of groundwater dynamics. From the view of hydraulics, almost all hydrogeologists have the opinion that the groundwater should be divided into two types of phreatic water and confined water.

In addition, due to the hydraulic properties of groundwater that mainly depend on the burial condition, some hydrogeological literature classified the groundwater according to the hydraulic properties referred to as buried groundwater types. The groundwater was divided into the three types of upper perched water, phreatic water, and confined water. Some literatures also added a groundwater type between two stratums. In fact the groundwater in aquifers between two aquicludes which do not have pressure head should also be the phreatic water from the view of hydraulic properties.

About groundwater classifications according to the aquifer medium, there are two kinds of classification schemes at present.

The first classification scheme origin from Soviet Union is used in Russia, China, and some other countries. The divided groundwater types are based on the gap types of aquifer medium. The basic idea of this classification is that there are completely corresponding relation between basic types of rock and gap types. A certain gap type (including intergranular pores, fracture, and corrosion pores) corresponds to a certain type of groundwater. According to this view, the groundwater can be divided into three classifications, namely pore water in loose uncemented rock, fissure water in non-soluble solid rock, and karst water in soluble rocks (limestone, dolomite, etc.). This classification can directly reflect the interdependent relationship among rock types, gap types of water storage, and the groundwater types (see Table 8.1). Therefore it becomes the theoretical basis for finding, exploration, evaluation of groundwater resources and has been widely used in hydrogeology textbooks and various rules of groundwater exploration, and hydrological geological scientific research and production.

The second classification scheme of groundwater classified by aqueous medium can be represented by the European and American countries, and can be seen in the book of *Hydrogeology* written by Davis and Dewiest (1966, USA), *Groundwater* written by R.A. Freeze and J.A. Cherry (1979, Canada), *Dynamics of Fluids in Porous Media* written by J. Bear (1979, Israel), *Groundwater Hydrology* written by H. Yamamoto (1992, Japan), and some other monographs. The types of groundwater are directly controlled by the rock types. Although there are no specific chapters about groundwater classification in these books, the characteristics of groundwater were all described based on the rock types of magmatic rock, metamorphic rock, volcanic, sedimentary rock (or further divided into sandy rock and carbonate rock), alluvium and permafrost rock types. The named aquifers also accord to the rock type (such as igneous rock and metamorphic rock aquifer,

Table 8.1 Aquifer classifications in bedrock

Rock types	Basic types of groundwater		Subclasses in rock types	Space types for water storage	Subclasses of groundwater	Names of the groundwater subclasses
Unconsolidated rock	Groundwater in unconsolidated rock (I)		Unconsolidated porous rock	Intergranular pore	Groundwater in unconsolidated porous rock (I_1)	Pore water
			Some loess and loess rocks	Intergranular pore, diagenetic pore and diagenetic fracture (vertical fissure)	Loess pore and fissure water (I_2)	Pore and fissure water
			Some clay	Diagenetic fracture (Consolidation)	Clay fissure water (I_3)	Clay fissure water
Half-hard rock	Bedrock groundwater	Half-hard rock groundwater (II)	Clastic rock of weak cementation	Pore between layers, bedding and structural fissures	Pore-fissure water in half cemented rocks (II)	Fissure-pore water
Insoluble solid rock		Groundwater in insoluble solid rock (III)	Basite volcanic ash layers of Cenozoic	The hole formed by diagenetic and weathering	Pore groundwater in volcanic ash (III_1)	Pore groundwater water in volcanic ash
			Basic lava (basalt) of Cenozoic	Diagenetic large holes and horizontal conduit	Groundwater in lava holes (III_2)	Groundwater in lava holes
			Insoluble solid rock	Tectonic, diagenetic and weathering fissures	Fissure water in bedrock (III_3)	Fissure water in bedrock (fissure water)
Soluble rock		Groundwater in soluble rock (IV)	Soluble rocks (various kinds of carbonate rocks and clastic rock with solute elements)	Tectonic rock fracture and fissure, cavity, caves of karst rock	Fissure-karst water (IV_1)	Fissure-karst water
			Soluble rock	Corrosion conduit and cave	Groundwater in corrosion conduit (IV_2)	Karst water

carbonate aquifer, clastic rock aquifer, etc.). The advantage of this classification scheme is intuitive, and easy to understand. But the rock types are various, thus the classifications of groundwater are multifarious and lack of systematicness. At the same time, this classification could not reflect the important hydrogeology properties, such as storage and transport of groundwater.

Compared to the above two kinds of groundwater classification schemes, it is obvious that the classification according to the rock gap types is more scientific. But in recent years, with the deepening development and exploration of the groundwater, the single groundwater classification scheme based on pore types of aqueous medium is still imperfect. There are several aspects as the following:

1. There is no absolute correspondence relation among the rock types, gap types, and groundwater types. For example, fracture gap is not only in the non-soluble solid rock. A large amount of fracture space can also exist in some loose rocks such as the loess and some kind of clay soils. Large-size space of holes is also not only in soluble carbonate rocks, but also in some of clastic rock with soluble components, such as cement or soluble breccia. Even there are various holes and conduits in volcanic rocks.
2. Some transitional rock types are among the three basic types of rocks (loose rock, the soluble solid rock, and soluble rock). They often have two types of space systems for water storage (i.e., double porosity media). There are many half cementation (hard) clastic rocks in Mesozoic and Cenozoic tertiary strata of China, which have both intergranular pores and diagenesis and the structural fissures. Thus both pore water and fissure groundwater exist in these rocks. Some clastic rocks with soluble compounds may have various space of diagenesis and the structural fissures, solution fissures and holes and even pipeline space, which contains both fissure water and karst water. The loess plateaus in northwestern China that both have pore water and fissure (vertical fissure) characterize as the dual-pore medium. For the present groundwater classification that based on aquifer medium types, the position of groundwater types in interim rocks and dual-pore medium is not clear.
3. During the groundwater exploration and development in recent years, some new types of water storage space were found. Water storage in large tunnel, shaft, and hole of the basic lava, and in some big holes layer of basalt (possibly the buried volcanic ash) also has great significance. However, these gaps and groundwater types in the current classification based on the general medium are in no position. In conclusion, the groundwater classifications simply according to rock types and its characteristics are not fit for the actual situation of groundwater existing forms and cannot summarize all groundwater types existed in nature. Therefore, the current widespread classification of groundwater is necessary to be further improved. The concepts of the three basic types of groundwater, especially the concept of fissure water also needs to be redefined.

Based on the above problems existing in the groundwater classification, Zisheng Liao added the interim type to the current three types, and named the groundwater

classifications reflected characteristics the rock and space types. The improved groundwater classifications (according to the classification of aquifer medium types) are shown in Table 8.1.

The basic features of this classification are as the following. First, the groundwater can be divided into two categories of "unconsolidated rock groundwater" and "bedrock groundwater" according to the structure characteristics of the rock. The bedrock groundwater can be further divided into three basic types of "half-hard rock groundwater," "groundwater in insoluble solid rock," and "groundwater in soluble rock" according to the rock structure and soluble features. Then according to the space characteristics of aquifer medium, unconsolidated rock groundwater can be further divided into three subclasses and the bedrock groundwater can be divided into six subclasses. Besides the traditional bedrock fissure water (III_3), this classification of bedrock fissure water actually includes the types of fissure-karst water (IV_1) in soluble rock and fissure-pore water in half-hard rock (II). Because fissure is the main space for the storage and transport of the three groundwater types, the regularity of groundwater movement and enrichment is mainly controlled by tectonic conditions. General bedrock fissure water, therefore, is the groundwater in hard and half-hard rocks and fissure is the main space for water storage.

8.2 Forming Conditions, Characteristics, and Storage Regularities of the Bedrock Fissure Water

8.2.1 Forming Conditions of the Bedrock Fissure Water

The formation, storage, and transport of the bedrock fissure water are influenced by various inside and outside factors. A combination of three basic conditions for the formation of bedrock fissure water is hard or half-hard rock, abundant water, and rock fissure resulted from the long-time tectonic movement.

Geological tectonism results in a large number of structural fissures in hard and half-hard rocks, which is the advantageous condition for groundwater storage and transport. The storage space for groundwater was formed at the fault fracture zone and its related fracture belt during the process that stratum or rock mass moved along the fracture surface. The intrusive body caused the deformation of surrounding rock at different rock contact zone, and fracture was formed or the original space of the fracture was increased. During the condensation of the dyke invasion and the influence of the later tectonic movement, a large number of protogenesis and secondary cracks was formed on dyke and both sides of the rock mass, providing favorable conditions for groundwater storage; Soluble rocks are mainly distributed in carbonatite area. The strong interaction would occur between carbonatite and hot water solution, resulting in the gradual increase of protogenesis and structural fissure and finally the various formations of karst structure.

8.2.2 Characteristics of the Bedrock Fissure Water

Distribution and movement of the bedrock fissure water (including buried karst water) has its uniqueness. Its main features are as follows:

1. The burial and distribution of bedrock fissure water are extremely uneven and are completely controlled by various kinds of fracture belts. Thus the aquifer is irregular.
2. The shape of the bedrock fissure aquifer is variety, and size and shape of the bedrock fissure are controlled by the geological structure and landform conditions. Thus burial and distribution condition of the bedrock fissure water are complex.
3. The bedrock fault vein aquifer buried deeply, but the quantity of groundwater is not abundant in normally.
4. The bedrock fissure water is obviously controlled by geological structure. The formation and distribution of various gaps in rocks are normally associated with the geological structure. Geological structure factor plays a leading role in the formation of the abundant aquifer in bedrock.
5. Dynamic properties of bedrock fissure water have their particularity. The groundwater buried in the same bedrock may not have the unified water table, and may alternately characterize as pressurized and confined water. Water movement is also complex, including laminar and turbulent flow. There may be pipe flow and open channel flow in the underground karst cave, which are not the forms of seepage flow. This is determined by the rock fissure and the special form of the karst cave.

8.2.3 Occurrence Regularity of the Bedrock Fissure Water

Occurrence regularity of the bedrock fissure water is the result of comprehensive shaping of many factors. Generally, lithology, geological structure, recharge, runoff and drainage, terrain, landform, and climate play a certain role in occurrence and distribution of the bedrock fissure water, and the lithology, structure, and supply factors play a main role.

The influence of lithology on bedrock fissure water is through the effective control on the fracture. The different mechanical properties of the rock develop the different size of the structural fissures under a certain tectonic stress. Take the plastic stratum for illustration, tectonic stress results in plastic deformation of the rock with the poor water occurrence. However, tectonic stress results in rupture of the brittle stratum with the rich water occurrence.

Under the effect of tectonic stress, various forms of deformation, such as fold and fault, are formed on the strata, increasing the space for water storage and the favorable conditions for water catchment. Due to the high fissures destiny of the

thin layered strata, the occurrence conditions for rich water are significant beneficial. For the thick-block strata, oblique stratifications are development with few and same scale fissures which are basically in closed state, and water occurrence conditions are poor. For the extraordinary development of the fracture structure, the squeeze fault resulted from squeeze and mylonitization is water-blocking, and cannot have the abundant groundwater. The faults with water occurrence and transport performed as water storage structures are usually extension or shear faults in the low class or order. These faults tend to have strong conductivity properties, but can't form a water-rich hose. As such, spatial variability of water occurrence condition was strong in the different parts of a fold. A certain scale of water-rich segment was usually formed at the wings of the anticline, steep turn slow parts of the stratum and syncline area under the negative terrain condition.

8.2.4 Flow Regularity of the Bedrock Fissure Water

The seepage of fissure water is much more complex than the pore water. The rock matrix of pore water is composed of particles with different sizes, and pores connect with each other between particles. Thus a unified free water surface can exist in the aquifer, and obey the Darcy's law for permeability. The fissure water is in the matrix of fractured rock. According to the distribution of structural planes, the fractured rock can be divided into five types: the whole structure, block structure, layered structure, fracture structure, and loose structure. In fact, the distribution of fractures in rock mass is inhomogenous, and some fissures are not connected. Thus the fissure water characterized as the shapes of slice, fasciculation, or vein. The permeability of the rock mass is controlled by the opening size of the fracture, geostress conditions and the rock properties.

Fractured rock mass is a multiphase discontinuous medium resulted from the incision of different scales, direction, and properties of the fissures due to the various geological processes. Geological structure, terrain, and hydrological factors resulted in the uneven and strong directional rock permeability for the fissure water with the extremely complicated seepage law.

1. Seepage law of fissure water in blocky rock mass

Blocky rock mass mainly refers to the rock mass with the relatively uniform properties, and has the blocky structure. The deep intrusive rocks, such as granite, and some volcanic and subvolcanic rocks are blocky rock masses. Except the strong tectonism areas, blocky rock mass general develops normal joint system and small fault with no regional fracture. However, the shear fractures are developed. The three kinds of the shear, squeezing, and tensile fractures are developed in the strong tectonism areas. Squeezing fractures have the weak permeability with no water occurrence. The permeability of shear fracture is medium. Tensile fracture has the high permeability with a large space for water storage.

In general, the permeability of rock mass is poorer with small space for water storage in blocky rock distribution area. Groundwater seepage in blocky rock mass depends on the structural plane (especially the fissure). Fissure development of the blocky rock mass is generally in weathered zone, fault or fracture zone, and intrusive contact zone.

2. Seepage law of the layered fractured rock mass

Layered rock mass mainly refers to the layered sedimentary rocks and sedimentary metamorphic rocks. The bedding, schistosity, and joint are developed in layered rock mass. The development characteristics and occurrence changes of the bedded fissures have a close relationship with the development degree of fold strata and stress condition.

(1) The thin layered rock mass is beneficial for water storage due to the high density of bedded fissures. Oblique beddings are developed in thick blocky rock mass with little quantity and small size of bedded fissures which are basically in closed state. Therefore, the water occurrence conditions are poor.
(2) For the same rock thickness, the plastic rock mass (clay rock, shale, marl, etc.) has the higher fissure density than the brittle rock mass (sandstone, limestone, igneous rock, etc.).
(3) For the stratums with bedding developed, anticlinal structure is beneficial for groundwater transport with the developed penetrability fissures. Groundwater often flows off to the two wings, and do not exist in axis of the anticline.
(4) The syncline structure is generally beneficial for water collection. If a tunnel locates at the syncline axis, it often encounters the relatively large amounts of water gushing. Fracture part in the shaft section of the syncline structure, which is called interlaminar fracture, is mainly deep embedded. When geostress worked on the stratum and the syncline was formed, the upper part of syncline structure was under the by maximum extrusion pressure, and the lower part under the tensile stress. Thus for the hard brittle stratum, the interlayer rock was breaked with the developed fissure joints. But for the argillaceous stratum, such as clay shale, the situation was different. Under the ideal circumstances of lithology, topography, geomorphology and climate, the interlaminar fractures in hard brittle stratum of the syncline of are favorable for groundwater accumulation.
(5) The seepage of fissure water in bedrock is along fissure networks of the strata with the characters of heterogeneity, anisotropy, orientation, and interaction with tectonic stress.

3. Seepage law of the cataclastic structured rock mass

Cataclastic structure mass was resulted from tectonic broken, fold broken of the rock, and interspersed extrusion of the magmatic rocks, joint, fault, fault infected zone, cleavage, bedding, schistosity, interlayer sliding surface, etc., are the main structural planes, developing the weak structural plane filled with some mud.

Groundwater is characterized as vein and fissure water, and often with local vein pressure.

The faults that have effects of block water are usually resulting from squeezing. Due to the extrusion and mylonitization, these faults are impossible occurrence of groundwater. However, the developed tensile or shear fractures at one or both sides of the fault effect zones are beneficial for groundwater occurrence. Tensile or shear faults with the properties of water transport and storage may form the local part for water rich, and sometimes with high-confined water head tend to have strong conductivity properties but no water-rich slices. If these faults communicate with the leaking limestone, fissure water of the sand and mudstone layer would be unwatering, and pore water in unconsolidated layer would be under the strong discharge with water table declining sharply.

4. Seepage law of unconsolidated structure

Unconsolidated structure is mainly fault fracture zone and strong weathering fracture zone resulted from tectonic action. Vein and pore water exist in the unconsolidated structure. Fracture rate at fracture surface or fracture zone of a single lithology, is usually higher in tensile fracture than in shear fracture, and squeezing fracture has the lowest fracture rate. The pure tensile fracture has the highest fracture rate. Thus, the squeezing fracture has the character of anti-water, but some parts of the fault may also be water rich. Tensile fracture is water rich, and tensile fracture is more beneficial for water storage. Water-rich capacity of the shear fracture is between the squeezing and tensile fracture.

8.3 Groundwater Seepage Model of Fractured Rock Mass

People have gradually realized the importance and urgency of fractured rock mass seepage since the arch dam break of Malpasset, French in 1959. Fractured rock mass seepage model is the basis of the fractured rock mass seepage analysis, although various fracture seepage models have been put forward, each one has its shortcomings. Perfect fractured rock mass permeability model still needs to be further established. Models of present mainly developed along the two directions, one was the fracture-pore dual-medium model considering the water exchange between fractures and matrix in the system, and the other was the non-dual-medium model which ignored the water exchange process.

8.3.1 Dual Model of Fracture-Pore

The dual-medium model of fracture-pore was considered that fractured rock mass is the unity formed by a fracture system with poor porosity but good hydraulic conductivity, and a pore system with good porosity but poor hydraulic conductivity.

It takes into account the water exchange process between the two kinds of systems. Fist, based on Darcy's law, water flow equations of the two medium systems were set up respectively. Then the water exchange equation connected the two separate flow equations. According to the established method, it can be divided into quasi-stable and unsteady flow models.

8.3.1.1 Quasi-stable Flow Model

The water exchange quantity of the fracture and pore rock system, which is implicit expression of time "*t*", is proportional to water head difference of the two systems for quasi-stable flow model. The main representative scholars of the model are Barenblattt, Warren and Rott, etc.

The concept of hydraulic dual medium was first put forward by Barenblatt with the main views as follows:.

(1) Fracture system and rock pore system are all throughout the region, forming an overlapping continuum. Each point of seepage field has two water head values, i.e., the average head value the pore system and the water head of fissure system.
(2) Permeability is several orders of magnitude smaller than the porosity of the rock. However, permeability of the fissures is several orders of magnitude larger than the porosity. Water flow in the rock mass is characterized by intense water exchange between the two different systems;
(3) It assumed that fissure and pore rocks are homogeneous and isotropic.

Although Barenblatt model was an important basis for the development of the dual-medium theory, the penetration mechanism of it was parochialism. Creak and pore system were all assumed to be the isotropic. Thus if the water exchange between two systems was ignored, the fractured rock mass could be seen as an isotropic porous media, and the desultorily fissures only worked as the pore channels. The extreme penetration mechanism may only appear in argillaceous rock affected by the intense tectonic movements, the rock mass suffered surface weathering. Therefore, the main disadvantage of Barenblatt model is that it did not reflect the anisotropic characteristics of the fractured rock medium and the fissure water flow.

Warren and Rott added new geometry and penetration restrictions to the assumptions of Barenblatt model of fissure system.

(1) Fissure system in rock mass is homogeneous, orthogonal, and interconnected. Permeability axis parallels to the orientation of fissure groups. Equal interval fracture groups with constant width are perpendicular to the main permeability axis. On the contrary, fracture groups along the main permeability axis may have various intervals and fissure widths for simulation of the anisotropy medium.

(2) The pore system divided by fissures is homogeneous and isotropic.
(3) Water exchange, which is proportional to the water head difference occurs between the two different systems, and water exchange quantity. Compared with Barenblatt model, the new model obviously considered the widespread anisotropy of permeability in fractured rock mass. However, it can only be applied to the uniform orthogonal fracture networks.

8.3.1.2 The Unsteady Flow Model

Unsteady flow model assumes that the process of water exchange of the two systems is the water in the pore system flows into the fracture system. According to the character of water flow in pore system, and the water exchange equation can be established. Due to the amount of water exchange is explicit formulation of time "*t*", it was called unsteady flow model. According to the space configuration of fracture system, the unsteady flow model present mainly includes parallel fractures unsteady flow model and the group fractures unsteady flow model.

The main assumptions in parallel fractures unsteady flow model are as follows:

(1) The fissure system is composed of a set of the width and interval of parallel fractures with infinite extension, and the rock was cut into columnar structures by fractures.
(2) The water exchange of the two systems is expressed as a vertical linear flow from pore system into the fracture system, which can be described by one-dimensional control equation with appropriate boundary and initial conditions. Obviously, the model is only appropriate for penetration space structure formed by the bedding fissure system.

The main assumptions of group fractures unsteady flow model are as follows:

(1) Fracture system consists of three intersection groups of fractures with the same crack width. The rock was cut into the massive body, and can be replaced with a series of equivalent homogeneous sphere with the same radius.
(2) Water exchange of the two systems is expressed as a radial flow from the center of rock matrix to the fracture. Compared to the parallel fractures unsteady flow model, this model obviously has made some improvements, but it still makes a certain restrictions on crack configuration.

The outstanding advantage of fracture-pore dual-medium model is that water exchange between the two different systems is considered, which is especially suitable for fluid storage in the fracture aquifer. The theory can be used for study of oil recovery from high pressure fractures of kilometers depth, or taking rare earth elements from ancient metamorphic water. However, for the two kinds of models based on this theory, the quasi-stable state flow model assumes that water exchange quantity is proportional to the he water head difference between the two systems, and is not directly explicit formulation of time "*t*" which would actually lead to big

error. Zimmerman pointed out that this error would eliminate only after a long time, and it cannot be ignored in the initial stage. For the unsteady flow model, water exchange equation is related to the space configuration of the fissure system. In order to establish water exchange equation, the configuration and shape of fissure system are made certain restrictions, which limit the application of these models. It should be noted that the conditions of fractures development should be considered in model selection for actual engineering. The fracture-pore dual-medium model remains to be further perfected.

8.3.2 Non-Dual-Medium Model

Another kind of model for fractured rock mass seepage analysis is the non-dual-medium model considering the fracture permeability. Due to ignoring water exchange between the pore and fissure system, it is not limited by rock mass fracture configuration when the model is applied, and it also can reflect the heterogeneous and anisotropic properties in fluid seepage. Thus, the non-dual-medium model is the most studied and widely used model at present. The non-dual-medium model mainly includes the equivalent continuum medium model, discrete fracture network model and the discrete coupling model which combines the advantages of the former two models.

8.3.2.1 Equivalent Continuum Medium Model

The fissure water is equivalent averaged to the entire rock mass, which can be characterized as an anisotropic continuum with a symmetric permeability tensor, and in the classical continuum theory is used in the equivalent continuum medium model.

The prominent advantage of equivalent continuous medium model is that anisotropic continuum theory which has solid foundation and experience both in theory and problem-solving methods can be used. What's more, the model can work without the exact location and hydraulic characteristics of each fracture, which is useful for those engineering problems with difficulty to obtain a single fissure data. However, equivalent continuous medium model has two difficulties in application. One is the determination of equivalent permeability tensor for fractured rock mass, and the other is that the effectiveness of the equivalent continuum model cannot be guaranteed.

1. Determination of the equivalent permeability tensor

A given equivalent permeability tensor must be unconditionally applied in the dynamic fields with similar water systems. Otherwise, the following questions will appear in determination of the equivalent permeability tensor. (1) The equivalent permeability tensor obtained in a certain boundary condition may not correctly

predict the flux through another boundary condition. (2) The equivalent permeability tensor decided by the flux may not be able to forecast the water head distribution accordingly. Therefore, when the model is applied to the fractured rock mass, the determination methods of the equivalent permeability tensor are very important.

Field water pressure test method, inversion method, and geometry method are the normal methods for determination of the equivalent permeability tensor.

(1) Water pressure test method. Because the permeability tensors of fractured rock mass have six independent parameters, a single-hole water pressure test is not sufficient to determine the permeability of fractured rock mass. In General, the permeability tensors of fractured rock mass in engineering are measured by three sections of water pressure test, group wells test, and cross wells of water pressure test. However, due to the large discrete degree of permeability of fractured rock mass, test results inevitably have the size effects. Considering the high cost of water pressure test, it cannot be performed in large area, so the field water pressure test is difficult to be applied widely.

(2) Inversion method. Inversion method is a kind of optimization methods. It determines the best collocation of divisional seepage parameters of rock mass based on the principle of the least difference between the analyzed and the tested groundwater table. The inversion method can be divided into two types: direct and indirect method. Due to the instability of direct method during calculating and high demands on the measured data, the indirect method is used more often. Inversion method is currently the most widely used method in engineering. However, because the permeability tensors of fractured rock mass have six independent parameters, determination of the permeability tensors may encounter the problems of nonuniqueness and instability. The selection of initial permeability parameter and some optimized coefficients is normally depended on the experience to a large extent, and inappropriate choice may not only affect the calculation speed but even the convergence of the results.

(3) Geometry method. Permeability of fractured rock mass mainly depends on the geometry parameters of fracture system, such as fracture azimuth, width and density of the fissures, etc., and also closely related to the size of the crack and connectivity. Therefore, for a known fracture system, geometry method can be used to determine the permeability tensors. For an actual rock mass, due to the random fracture distribution, statistical analysis on the fractures is needed firstly to divide the fractures into several groups with typical fracture surface, and then the equivalent permeability tensors can be obtained. Because it is difficult to measure the geometry parameters of fissure system accurately in engineering, and also difficult to quantify the influence of crack size and connectivity on the permeability tensor of rock mass, geometry method can only determine the initial value of permeability tensor which should be finally corrected by hydraulic test or inversion method.

2. Effectiveness of the equivalent continuum model
Whether the continuum seepage theory can be used to analyze the fractured rock mass seepage is a controversial issue. Many scholars have put forward some criterions. Louis gave a view that for an engineering rock mass, when the number of fractures in rock mass is more than 1000, the equivalent continuous medium model can be used. Maini found that if the ratio of average crack spacing of rock mass and building size was less than 1/20, the equivalent continuum model can be used. In the study by Wilson and Witherspoon, the ratio of largest joint spacing of the rock mass and the construction size is less than 1/50 is the criterion of using equivalent continuum model. But all these criterions are obtained from the specific project or theory analysis, and they are difficult to be applied in actual engineering.

Long did the further research, and pointed out that two conditions were needed to characterize the fractured rock mass as a continuous media.

(1) Sample volume is suitable for simulation, i.e., equivalent permeability only has a small change with the slight increase or decrease of the size of test body.
(2) The symmetrical equivalent permeability tensors, which can be determined by the measured directional permeability, exist in the fractured rock mass. Supposing K_J as the permeability in hydraulic gradient direction and K_f as the permeability in flow direction, if $K_J^{1/2}$ and $K_f^{1/2}$ can be plotted as an ellipse in polar coordinates, the medium should have symmetrical permeability tensors. In addition, the effect of fracture geometry parameters on fissure permeability was also studied by Long. He gave the view that the random distribution of fracture directions and the constant crack width are beneficial to the effectiveness of the equivalent continuum model. The fracture rock mass with more intensive fracture networks, resulting a better connectivity, is more close to an equivalent anisotropic continuum medium.

8.3.2.2 The Discrete Fracture Network Model

Discrete fracture network model is on the premise of figuring out every spatial orientation, gap width of crack geometry parameters, and is based on the basic flow formula in a single fissure. It uses the principle of equal quantity between inflows and outflows of each fracture intersection to establish the equation and then by solving equations to obtain the crack head value of the intersection.

The network line element method was first put forward by Wittke and Louis, which is similar to loop the current method in circuit analysis. Mao Changxi described a crack hydraulic network model similar to pipe network of hydraulics. Wilson and Witherspoon simulated the fissures in rock mass using triangular elements or line units respectively. They showed a finite element technology to simulate the two-dimensional fracture network flow, and demonstrated that interference of fracture cross-flow can be neglected in an example to illustrate the advantages

and feasibility of the line unit method. For the three-dimensional problems, a three-dimensional fracture network disk model was first put forward by Long, solved by the hybrid analytical–numerical method. Nordqvist showed a three-dimensional network model with the metabolic fracture width. Dershowitz described a three-dimensional polygonal fracture network model. In further research, Wanli combined it with the finite element method, and showed a polygon unit seepage model of three-dimensional fracture network.

In these methods of solving three-dimensional problems, finite element method is most effective and convenient to simulate the discrete fracture network. If the fracture cross interference flow can be neglected, for saving calculation, graphic element can be used to simulate fracture surface, and surface intersections will be the nodes. Thus the two-dimensional flow on the local surfaces of fracture network forms the overall three-dimensional flow. Because crack units are not on the same plane, first of all local coordinate system *o'x'y'* for each fracture unit should be set up. In the local coordinate system *o'x'y'*, the cracks flow can be regarded as local two-dimensional isotropic flow. Then finite element control equation $[K]^e h^e = F^e$ of each fracture unit can be established respectively. According to flow balance in the node of fracture intersections, i.e., $\sum_e F^e \cdot b = 0$, the integral finite element equation is obtained.

It shows that the discrete fracture network model gives a specific simulation on each fracture in the network system and tries to get real seepage state of each point in the fissure system, which obviously has good simulation and high precision. However, when the number of fissures is large, the workload is tremendous or even impossible, especially for the three-dimensional problems. In addition, due to the randomness of fracture distribution, to establish a discrete real fissure system is also very difficult. Therefore, except the simple condition, it's difficult to use discrete fracture network model widely d in actual engineering.

8.3.2.3 Equivalent Discrete Coupling Model

Equivalent discrete coupling model is a new model combined with the advantages of equivalent continuous medium model and discrete fracture network model. As proposed above, discrete fracture network is characterized as the good simulation and high precision, but tremendous workload for simulation of larger number of fissures. Equivalent continuum model can overcome the difficulties, but its effectiveness is difficult to guarantee when fissure density is small. Thus, some scholars put forward a coupling model with combining of the above two models. A partition mixture model can be described as follow. Discrete fracture network model is used for the fracture areas with smaller fissure density and equivalent continuum model is used for large fissure density areas. The unified domain mixed model can be used for the an area that the discrete fracture network model is used for simulation of a few large and medium-sized cracks fissures which play an important part in permeability adopt, the equivalent continuum model is used for simulation of large destiny small cracks in the blocks divided by large or medium-sized cracks. Then coupling discrete equation can be established according to the equal heads

(i.e., unified head) and node flow balance in the connected areas of the two medium types. This model with enough engineering precision can not only obviously avoid the huge workload in discrete fracture network model for simulating each fracture, but also guarantee the effectiveness of the equivalent continuum model.

8.4 Three-Dimensional Numerical Model for Bedrock Fissure Water

Adopting model technology into study on the migration regularity of groundwater in the rock mass is of great significance for analyzing the seepage law of fissure water, the calculation and evaluation of water resources, the seepage field analysis and forecast, and so on. Building a mathematical model to reflect the migration regularity of real fissure water in the space is still a difficult problem. A comprehensive model which has coupled a one-dimensional flow model specifically reflecting the flow in a water channel and a three-dimensional numerical model reflecting the seepage of fractured rock mass, which can also link the water corridor model in turbulent flow condition, has a practical meaning.

Fissure water model research began in the 1960s, and a certain amount of progress has been made. The study mainly developed along two directions. One is the double-medium model, but the establishment of the model needs to make some assumptions for the fissure and rock mass system, which limits its application. Another is the double-medium model, mainly includes the discrete medium model and equivalent continuum model. Building a discrete medium model requires the geometrical characteristics and permeability coefficients of all the fissures for transporting water. As its difficulty and big workload, it is hard to apply in practical. Widely used equivalent continuous medium model can simulate the fractured rock mass with symmetrical permeability tensors of anisotropic body, and the mature continuum theory can be used. At present, it is mainly applied in two-dimensional flow model, and few researches were about the three-dimensional flow model. Also, the equivalent continuum model is not always effective.

According to the research status of fissure water numerical models, the equivalent coupling continuum model based on the equivalent continuous theory, reflecting the one-dimensional linear flow in a transport channel and the three-dimensional of the seepage in fractured rock mass, and coupling water sink gallery model of the non-Darcy flow, should be established. It is valuable and important to seek effective solving method for coupling model, and make the research results into practical applications.

The fissure development characteristics are the main factors influencing the fissure water transport. Fissure water flows in the complex networks composed of banded faults, planar apertures and tubular and cavern fissures. Specially, the tubular fractures usually play a role of water corridor and transport channel. Thus, the vein seepage characteristics of fissure water are that the water mainly transports in the trunk fractures and stores in the microcracks and blowholes. Fissure water

flow of the high heterogeneity and anisotropy, is generally the laminar flow in rock mass and conforms to the linear Darcy's law. However, there may be turbulent flows at the large space such as the karst channels.

According to characteristics of fissure water seepage, a coupling model was put forward for the three-dimensional flow. One-dimensional flow model based on the local coordinate system was established for specific simulation of water flow in the transport channels of fractured rock mass. Water exchange model was established for the turbulent state of flow in water transport channels. But for the whole fractured rock mass system with small scale and large density of fissures, the three-dimensional flow model should be established.

8.4.1 Equivalent Three-Dimensional Model

$$\begin{array}{ll} \frac{\partial}{\partial x}\left(K_{xx}\frac{\partial h}{\partial x}\right)+\frac{\partial}{\partial y}\left(K_{yy}\frac{\partial h}{\partial y}\right)+\frac{\partial}{\partial z}\left(K_{zz}\frac{\partial h}{\partial z}\right)-W=\mu_s\frac{\partial h}{\partial t} & (x,y,z)\in G, t\geq 0 \\ h(x,y,z,t)=h_0(x,y,z) & (x,y,z)\in G, t=0, \\ h(x,y,z,t)|_{\Gamma_1}=h_1(x,y,z,t) & (x,y,z)\in \Gamma_1, t\geq 0 \\ [K]\mathrm{grad}h\cdot n|_{\Gamma_2}=q(x,y,z,t) & (x,y,z)\in \Gamma_2, t\geq 0 \end{array} \tag{8.1}$$

where h is the groundwater head, L; μ_s is the specific storage of fracture media, L^{-1}; K is the equivalent anisotropic hydraulic conductivity, LT^{-1}; n is the unit outside normal vector of the boundary.

$$W=\sum_{j=1}^{N_w}\sum_{k=1}^{N_L}Q_{jk}\delta(x-x_j,y-y_j,z-z_{jk}) \tag{8.2}$$

where N_w is the number of pumping wells; N_L is the number of the layers; Q_{jk} is the water yield of the kth layer and jth well.

8.4.2 One-Dimensional Model

$$\begin{array}{ll} \frac{\partial}{\partial x}\left(K_x\frac{\partial h}{\partial x}\right)+Q=\mu\frac{\mathrm{d}h}{\mathrm{d}t} & (0\leq x\leq L, t>0) \\ h|_{t=0}=h_0(x) & (0\leq x\leq L) \\ h|_{x=0}=f_1(t), h|_{x=l}=f_2(t) & (t>0) \end{array} \tag{8.3}$$

where h is the water transport channel; Q is recharge-source; K_x is the permeability coefficient along the fracture, LT^{-1}, $K=\frac{b^2\rho g}{\lambda\mu}$; μ is water release coefficient of the fractured medium (dimensionless); t is the time; T, x is the local coordinates along the fracture.

8.4.3 Water Catchment Corridor Model

The approximate calculation formula for water discharge considering the inside and outside water head difference of water transport channel and the conductivity performance between rock masses can be expressed as:

$$Q \approx T(h - d) \tag{8.4}$$

where Q is the inflow of water transport channel, L^3T^{-1}; h and d are the water heads of fractured rock mass and water transport channel, respectively, L; T is the transmissibility coefficient of the interface of fractured rock mass and water transport channel, L^2T^{-1}.

Based on principle of the of water head continuity at interface of water transport channel and the overall system of rock mass, and the flow equilibrium at unit nodes of the according parts, the coupling of two kinds of medium models is as the following. The respective permeation unit matrixes of two medium models were formed after the discretization of the partial differential equation. According to the principle of unified node number at the interface of the two kinds of medium, permeation unit matrixes of two medium were superposed to form the overall seepage matrix without having to make other transformation. Water exchange model of the turbulent water catchment corridor can be superposed to the overall matrix according to the unit node numbers of water catchment corridor. The algebraic equation of coupling seepage model of the fractured rock mass was obtained on the basis of above assembling. During the process of forming calculation program, the overall matrix of coupling model can be formed by cumsum with the same node number. The finally formed large algebraic equations can be solved by strong implicit iteration method with well stability.

8.5 Project Types and Instances of Bedrock Fissure Water

8.5.1 Groundwater of the Rock Slope Engineering

8.5.1.1 The Effects of Groundwater on the Rock Slope Stability

Groundwater has important effects on slope stability, especially on the reservoir bank slope. The influence of groundwater on the slope stability is mainly manifested in the following three aspects:

1. The influence of groundwater soil physical and mechanical properties of the slope rock

On the one hand, the saturated rock was soft after reservoir impoundment. Friction coefficient and cementing ability of the soil particles are lower as a result of the water lubrication. Shear parameters of the potential sliding surface are reduced,

decreasing slope sliding resistance. On the other hand, during the reservoir operation, repeat rise and fall of the water table result in cycle seepage flow in the slope body. Groundwater seepage has the leached effects on slope, and the tiny particles also transport under the action of groundwater. Slope erosion phenomenon, the mesoscopic and macroscopic cavities on the potential sliding surface of slope body, reduce shear strength of the potential sliding surface.

2. Buoyancy

Rock body immersed in reservoir water is under the buoyancy effect of groundwater. Buoyancy is equal to the product of underwater rock volume and water weight of per unit volume, i.e., $A_w\gamma_w$. In general, the weight of underwater slope is equal to its weight under buoyancy. There are two aspects of buoyancy on the slope stability. On the one hand, buoyancy reduces the effective weight of the slope body. The sliding resistance of the sliding surface is reduced, which brings adverse effect to the slope stability. On the other hand, the weight decrease of the slope body reduces the slide force, contributing to the slope stability. Therefore, stability evaluation of the buoyancy on slope is not simply the pros and cons, and should consider the specific engineering geological conditions and comprehensive evaluation of mechanical parameters of the rock–soil body.

3. Seepage force

Instability of many slopes occurred while the reservoir water table dropped sharply. One reason for this was that the disappearance of the buoyancy increased effective weight of according part of the slope, leading to changes in slope stability. The other reason is that the dropped water table resulted seepage flow in rock–soil body, and the seepage force caused the slope unstability. The seepage force was controlled by shape of the saturation line, the permeability coefficient of the rock mass, the size of saturated area and dip angle the potential sliding surface, etc. Currently, there is no accurate calculation method for seepage force. The saturation line of slope body is complex to determine, is affected by permeability coefficient and specific yield of the rock and dropping speed of the reservoir water table. According to *The Engineering Handbook of Foundation Pit*, the average hydraulic grade is used for calculating the seepage force. And the average hydraulic grade is slope of the line connected the intersection points of saturation line and the landslide mass slope (as shown in Fig. 8.1, the slop of the AB line). The total seepage T of slide body can be calculated by the following equation:

$$T = \gamma_w A_w I \tag{8.5}$$

where γ_w is the water weight of per unit volume; A_w is the area beneath the saturated line; I is the average hydraulic grade.

Seepage force is along the direction of average hydraulic grade. Although the calculation of the hydraulic gradient is simplified in Eq. (8.5), the shape of the saturation line should be determined to calculate the saturated area. Thus the Eq. (8.5) is more suitable for the circular sliding surface. Transfer coefficient

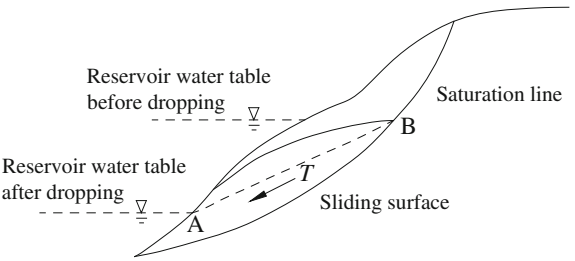

Fig. 8.1 Schematic of the hydraulic gradient for a slope

method can be used to analyze the slope stability. For the slip surface shaped as broken line, based on the simplified and safety consideration after the reservoir water table decline, the slope line is generally assumed to be the saturation line. Assuming the direction of seepage force is sliding surface tangential, the seepage force can be expressed as:

$$D_i = \gamma_w A_w \sin \omega_i \tag{8.6}$$

where D_i is the seepage force of the ith slice; ω_i is the dip angle of the ith slice.

8.5.1.2 Calculation Model of the Slope Stability, Considering the Role of Groundwater

Engineering stability of rock slope can be calculated by various methods, such as the finite element method, probability method and limit equilibrium method, and so on. However, the limit equilibrium method is the most commonly used method, and is described below for the broken line sliding surface.

Residual sliding force and stability coefficient of the slop are calculated by the transfer coefficient method. According to the broken line shape of the sliding surface, the sliding body is divided into vertical bars at line turning points of the broken line (Fig. 8.2). The transfer coefficient for the residual force of the vertical bars from top to down is expressed as:

$$\lambda_i = \cos(\omega_i - \omega_{i+1}) - \sin(\omega_i - \omega_{i+1}) \tan \varphi_i \tag{8.7}$$

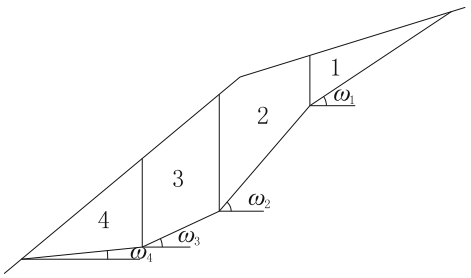

Fig. 8.2 Schematic of slice method for the slop

where λ_i is the transfer coefficient passed from residual sliding force of the ith slice to the $(i + 1)$th slice; φ_i is the friction angle of sliding surface of the ith slice, which is the saturated friction angle when soil is saturated.

Thus, the residual sliding force passed from the ith slice to the $(i + 1)$th slice can be expressed as:

$$E'_{i+1} = \lambda_i E_i \tag{8.8}$$

Obviously, if $E_i \leq 0$, indicated there is no residual sliding force for the ith slice. Stability coefficient and slide thrust of the slope can be calculated as follows:

$$F_s = \frac{\sum_{i=1}^{n-1}\left(R_i \prod_{j=1}^{n-1} \lambda_j + R_n\right)}{\sum_{i=1}^{n-1}\left(T_i \prod_{j=1}^{n-1} \lambda_j + T_n\right)} \tag{8.9}$$

$$E_i = \lambda_{i-1} E_{i-1} + K_s T_i - R_i \tag{8.10}$$

$$R_i = W_i \cos\overline{\omega_i} \tan\varphi_i + c_i L_i \tag{8.11}$$

$$T_i = W_i \sin\overline{\omega_i} + D_i \tag{8.12}$$

$$D_i = \gamma_w A_w \sin\overline{\omega_i} \tag{8.13}$$

where F_s is stability coefficient of the slope; R_i is the sliding resistance for the ith slice; K_s is the designed security coefficient of the slope; T_i is the sliding force of the ith slice; W_i is the weight of the ith slice, in which submerged weight should be used when it is under saturated condition; c_i is the cohesion of the sliding surface of the ith slice, in which saturated cohesion should be used for the saturated slope; L_i is the length of the sliding surface for the ith slice.

Equations (8.9) and (8.10) reflect the comprehensive influence of the groundwater on the stability of the slope, such as the change of the mechanical parameters of sliding surface, buoyancy, seepage force, etc. From the two formulas, we can get two criterions on the slope stability. If $F_s \geq K_s$, the slope is stable, otherwise is unstable. If $E_n \leq 0$, the slope is stable, otherwise is unstable.

8.5.1.3 Stability Seepage Force of the Landslide

1. The basic concept

Landslide stability analysis is based on Mohr–Coulomb theory. The main two methods for landslide stability analysis are the total stress method (Su-analysis) with the consideration of the undrained shear strength (Eq. 8.14), and effective

stress method ($\overline{c}$ and $\overline{\varphi}$ analysis) with the consideration of the drainage shear strength (Eq. 8.15).

$$K_{\mathrm{f}} = \frac{\sum (N_i \tan \varphi_i + c_i L_i)}{\sum (W_i \sin \alpha_i)} \tag{8.14}$$

$$K_{\mathrm{f}} = \frac{\sum (\overline{N}_i \tan \overline{\varphi}_i + \overline{c}_i L_i)}{\sum (W_i \sin \alpha_i)} \tag{8.15}$$

Look from the quantity, the difference between the two methods is that pore water pressure of the sliding zone is considered in the $\overline{c}$ and $\overline{\varphi}$ analysis method. The pressure is equal to h_{w}, the height the slide body beneath infiltrate surface, multiplied by γ_{w}, the weight of per unit volume water. For any vertical slice of the slope with the width of l_i, the effective normal stress $\overline{N}_i$ is equal to the total normal pressure, N_i minus pore water pressure, or as $N_i = \overline{N}_i - \gamma_{\mathrm{w}i} h_{\mathrm{w}i} l_i$.

However, from the intrinsic view, the seepage effect and declined water table are considered in the $\overline{c}$ and $\overline{\varphi}$ analysis method. The pore water pressure is deducted, thus the sliding resistance is produced by the effective stress completely in the stability analysis. This method is more suitable for the stability evaluation of accumulated layer landslide under long-term changes of water table. Taking the Three Gorges Project as an example, Most of the slopes influenced by the changes of reservoir water table are accumulated layer landslides. Continuous infiltration surface, i.e., a unity of underground water table, is normally formed by the control of reservoir water table. Long-term stability is the main goal of the landslide stability analysis. Thus, the effective stress method should be used for this.

According to Bernoulli equation, the total water head of the seepage flow of the saturated soil water is the sum of position head, pressure head, and flow velocity head. The sum of the position head and the pressure head is called the piezometric head. In general, the velocity head can be neglected in landslide because of the large soil seepage resistance and the velocity flow. Total stress can be considered to be the sum of the effective stress and buoyancy of the sliding body skeleton. However, the sharply decline of the water table and also its movements from the range of 175–145 m exist in Three Gorges reservoir area. The total head (equivalent to the piezometric head) of different parts of the main landslide section would decrease along the flow direction. The ratio between the head loss, Δh of the two points and the penetration length, L, is named as the hydraulic slope, I. Therefore, the seepage force which is the external force of water flow on soil slope should be considered, namely. Seepage force is a kind of volume force. It is proportional to the hydraulic grade, and has the same direction as the seepage.

2. Calculation formulas for the landslide stability coefficient and thrust under the seepage pressure

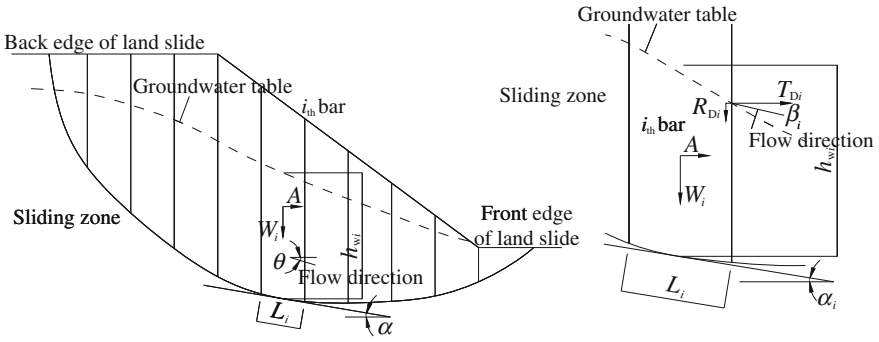

Fig. 8.3 A calculation model of accumulated layer landslides: Sweden slice method (*circular sliding* surface)

In general, the shapes of sliding zone of reservoir landslide are circular arc and broken lines with the corresponding calculation models:

(1) Sliding surface as a single plane or arc surface (Fig. 8.3) landslide stability calculation:

$$K_{\mathrm{f}} = \frac{\sum \left((W_i(\cos \alpha_i - A \sin \alpha_i) - N_{\mathrm{w}i} - R_{\mathrm{D}i}) \tan \varphi_i + c_i L_i \right)}{\sum \left(W_i(\sin \alpha_i + A \cos \alpha_i) + T_{\mathrm{D}i} \right)} \tag{8.16}$$

where $N_{\mathrm{w}i} = \gamma_{\mathrm{w}i} h_{\mathrm{w}i} L_i$ is pore water pressure, which is approximately equal to the area beneath the infiltration plane $h_{\mathrm{w}i} L_i$ multiplied by the weight of per unit volume water γ_{w}.

Component force of the parallel sliding slice resulted from the seepage force is expressed as:

$$T_{\mathrm{D}i} = \gamma_{\mathrm{w}} h_{\mathrm{w}i} L_i \sin \beta_i \cos(\alpha_i - \beta_i)$$

Component force of the vertical sliding slice resulted from the seepage force is expressed as:

$$R_{\mathrm{D}i} = \gamma_{\mathrm{w}} h_{\mathrm{w}i} L_i \sin \beta_i \cos(\alpha_i - \beta_i)$$

where W_i is the weight of the ith slice, kN/m; c_i is the cohesion of the ith slice, kPa; φ_i is the internal friction of the ith slice, °; L_i is the sliding length of the ith slice, m; α_i is the first slide angle of the ith slice, °; β_i is the groundwater flow direction of the ith slice, °; A is coefficient of the earthquake acceleration (gravity acceleration, g); K_j is the stability coefficient.

It's very difficult to determine the pore water pressure of the landslide. The effective stress can be assumed as:

$$\overline{N}_i = N_i - \gamma_{wi} h_{wi} l_i = (1 - r_U) W_i \cos \alpha_i$$

where r_U is the pore pressure ratio, defined as the ratio of the total pore water pressure and total uplifting pressure, can be expressed as:

$$r_U = \frac{\text{Underwater area of the sliding body} \times \text{unit water weight}}{\text{Total volume of the sliding body} \times \text{unit sliding body weight}} \approx \frac{\text{Underwater area of the sliding body}}{\text{Total area of the sliding body} \times 2}$$

In general, the ratio of unit water weight and unit sliding body weight is reduced to 0.5. Thus, r_U is greatly simplified in calculation by the total underwater area of the slices.

Accordingly, Eq. (8.16) can be simplified as:

$$K_f = \frac{\sum \left(\left(W_i (1 - r_U) \cos \alpha_i - A \sin \alpha_i \right) - R_{Di} \right) \tan \varphi_i + c_i L_i \right)}{\sum \left(W_i (\sin \alpha_i + A \cos \alpha_i) + T_{Di} \right)}$$

where W_i is the weight of the ith slice, kN/m. Different slope layers which may have various weights must be considered in the calculation. The slop body weight of above and under the seepage surface should also be distinguished, with the natural weight above the water table and saturated weight under the water table, and can be expressed as:

$$W_i = (\gamma_i h_{1i} + \gamma_{sat} h_{wi}) b_i$$

where γ_i and γ_{sat} are the natural and saturated weight of the slope respectively; h_{1i} and h_{wi} are the heights of the vertical slice above and under the seepage surface respectively. It should be noted that due to considering of the static pore water pressure, submerged weight γ' is not used in the formula. If submerged weight is considered, i.e., $\gamma' = \lambda_{sat} \gamma_w$, the pore water pressure N_{wi} should be merged in Eq. (8.16).

Accordingly, Eq. (8.16) can be transformed as:

$$K_f = \frac{\sum \left((W_i (\cos \alpha_i - A \sin \alpha_i) - R_{Di}) \tan \varphi_i + c_i L_i \right)}{\sum \left(W_i (\sin \alpha_i + A \cos \alpha_i) + T_{Di} \right)} \tag{8.17}$$

Calculation the landslide thrust

Shen Runzhi et al. proposed a calculation formula of the landslide thrust based on arc method. According to the characteristics of the slop and the prevention and treatment engineering, two calculation methods for thrust are proposed.

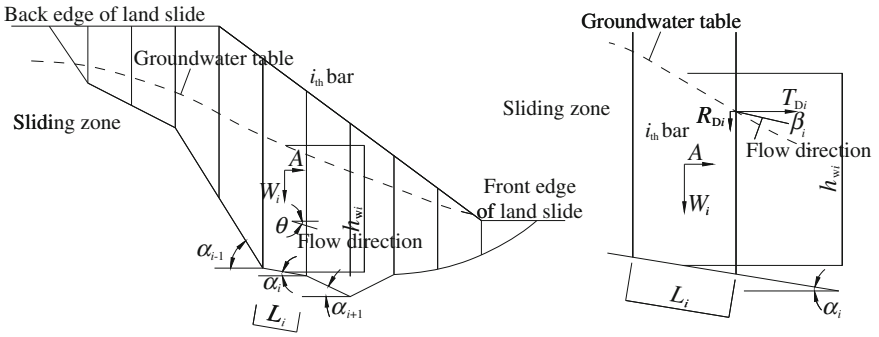

Fig. 8.4 Landslide model II: transfer coefficient method (*broken line* surface)

Shear resistant: the sliding body is relatively intact and intensity, and the shearing strength of the sliding slice is low. The landslide thrust is general in rectangular distribution.

$$H_s = (K_s - K_f) \times \sum (T_i \times \cos \alpha_i) \tag{8.18}$$

Bending resistance: sliding body integrity is poor. The landslide thrust is general in triangular distribution.

$$H_m = (K_s - K_f)/K_s \times \sum (T_i \times \cos \alpha_i) \tag{8.19}$$

where H_s and H_m are the landslide thrust, kN; K_s is the designed safety coefficient; T_i is the tangent force component of the vertical slice weight in sliding zone.

(2) The sliding surface is as broken lines shape (Fig. 8.4)

(1) Calculation of the landslide stability

$$K_f = \frac{\sum_{i=1}^{n-1} \left[((W_i((1 - r_U)\cos \alpha_i - A \sin \alpha_i) - R_{Di}) \tan \varphi_i + c_i L_i) \prod_{j=i}^{n-1} \psi_j \right] + R_n}{\sum_{i=1}^{n-1} \left[(W_i(\sin \alpha_i + A \cos \alpha_i) + T_{Di}) \prod_{j=i}^{n-1} \psi_j \right] + T_n} \tag{8.20}$$

where $R_n = (W_n((1 - r_U)\cos \alpha_n - A \sin \alpha_n) - R_{Dn}) \tan \varphi_n + c_n L_n$

$$T_n = W_n(\sin \alpha_n + A \cos \alpha_n) + T_{Dn}$$

$$\prod_{j=i}^{n-1} \psi_j = \psi_i \psi_{i+1} \psi_{i+2} \cdot \ldots \cdot \psi_{n-1}$$

where ψ_j is the transfer coefficient passed from residual sliding force of the ith slice to the $(i + 1)$th slice, and can be expressed as:

$$\psi_j = \cos(\alpha_i - \alpha_{i+1}) - \sin(\alpha_i - \alpha_{i+1}) \tan \varphi_{i+1}$$

The notes are the same as above.

(2) The landslide thrust

The calculation formula for landslide thrust based on the transfer coefficient method can be expressed as:

$$P_i = P_{i-1} \times \psi + K_s \times T_i - R_i \tag{8.21}$$

where sliding force is

$$T_i = W_i \sin \alpha_i + A \cos \alpha_i + \gamma_w h_{wi} L_i \tan \beta_i \cos(\alpha_i - \beta_i);$$

sliding resistance is

$$R_i = (W_i(\cos \alpha_i - A \sin \alpha_i) - N_{wi} - \gamma_w h_{wi} L_i \tan \beta_i \sin(\alpha_i - \beta_i)) \tan \varphi_i + c_i L_i;$$

transfer coefficient is

$$\psi = \cos(\alpha_{i-1} - \alpha_i) - \sin(\alpha_{i-1} - \alpha_i) \tan \varphi_i.$$

Considering the pore water pressure ratio, sliding resistance R_i can be calculated by the following formula:

$$R_i = (W_i((1 - r_U) \cos \alpha_i - A \sin \alpha_i) - \gamma_w h_{wi}) \tan \varphi_i + c_i L_i$$

(3) Working condition of landslide prevention design discussion

In general, dead weight is the basic load of the landslide, and rainstorm and earthquake are the exceptional loads. Taking the prevention and treatment engineering of Three Gorges Reservoir as an example, the load type is closely related to the changes of the reservoir water table.

After the buildup of the Three Gorges Reservoir, the water table before dam is at 145–175–145 m between in flood season (October to early April of the following year), and has a 30 m variation range. When the reservoir works in flood season (middle of June to the end of September), the reservoir storage table must be reduced to flood limit water table of 145 m to held the occurred flood. For once a flood in 5a, 20a, 100a and 1000a, water tables before dam must keep at 147.2 m, 157.5 m, 166.7 m and 175 m respectively. The reservoir water table would quickly decrease to 145 m after the flood peak to prevent flood occur again. Thus from the

safety consideration, water table sharply declines from 175–145 m can a working condition for checking.

For the working condition, the dead weight would serve as a temporary base load which would be ended in 2009, and dead weight added with the rainstorm would also be the temporary exceptional load. These two kinds of load would not serve as the designed working conditions of the landslide prevention and control engineering affected by the reservoir for the Three Gorges Reservoir area.

Dead weight added with reservoir water table of 175 m should be the basic load of the Three Gorges Reservoir area. The second phase water table of 135 and 156 m for the transition are not as a design conditions into consideration. Corresponding with this, dead weight and rainstorm added with water table of 175 m, dead weight added with water table range of 175–145 m, and dead weight and rainstorm added with water table range of 175–145 m should serve as the working conditions of landslide design for engineering design and check. Because the reservoir is in weak seismic activity area, the general working condition of landslide control engineering does not consider the earthquake.

Due to the rapid development of many immigrant towns in the reservoir area in recent years, the construction land shortage is serious. Many houses, even the tall buildings, have to be built on landslide. Thus building load should be as a kind of working condition, or converted into the added dead weight, in these landslide areas. Specially, the load or overload (even several times) of the track should be considered at prevention and control engineering in riverside road areas.

8.5.1.4 Calculation of Slope Stability

The Three Gorges Project is famous in the world due to large storage capacity, long returning flow, and high water table fall. It could be ensured after putting completed reservoir into use that the normal water table in the front of dam is 175 m and limited water table for flood prevention is 145 m, indicating that the amplitude of variation is 30 m. The hydrogeological conditions in reservoir area are strongly affected because of water cycle fluctuation, resulting in deteriorated rock and soil mechanics features of slope body and large hydrostatic pressure and seepage force, which in turn cause revival of old landslide and buckling failure of current stable slope. As a result, these problems may bring a security risk on human life and property, and operation of the reservoir. Taking Guantangkou landslide of Wanzhou, Chongqing as an example, the effects of groundwater in bedrock area on slope stability are detailed introduced and further evaluated.

Case 1: **Landslide of Guantangkou in Wanzhou, Chongqing**

1. Basic characteristics of Guantangkou Landslide

(1) Geological conditions

Shown as Fig. 8.5, landslide area is located at right bank slope of Zhuxi River in Wanzhou, and it has a landscape of medium hills, river valley, and bank slope. It is also a part of the Taibai rock old collapse body slide. The elevation at right is higher than that at left and top elevation ranges from 212 to 222 m, 80 m higher than Zhuxi River. Landslide distributes along the rolling erosion gully. The terrain shows a step type, and the surface slope at top is steeper than that at bottom. The top landslide, which is demarcated by Guoben branch road is a slope with a slope angle of 25°–35°. The bottom landslide is a rank-2 slope with a small slope angle of 5°–10°. And it extends to Zhuxi River, which becomes incongruous. The table-board elevation of rank-1 step from south to north ranges from 160 to 177 m, and width ranges from 140 to 260 m. The table-board elevation of rank-2 slope ranges from 140 to 160 m, and width ranges from 80 to 150 m. A slope or scarp connects the slope of rank-1 and rank-2 with a slope angle of 10°–25° and scarp height of 3–10 m. Band slope of front exit is along with the river with a height of 8–16 m, and a slope angle of 20°–50°.

Landslide group of Guantangkou shows a type of a short boot and its elevation of south is higher than that in north. Back edge elevation ranges from 212 to 222 m, front exit elevation ranges from 133 to 141 m and the difference is 80 m. Furthermore, the length between south and north is about 500 m, width between east and west is about 800 m, and thickness ranges from 17.0 to 49.1 m. The total

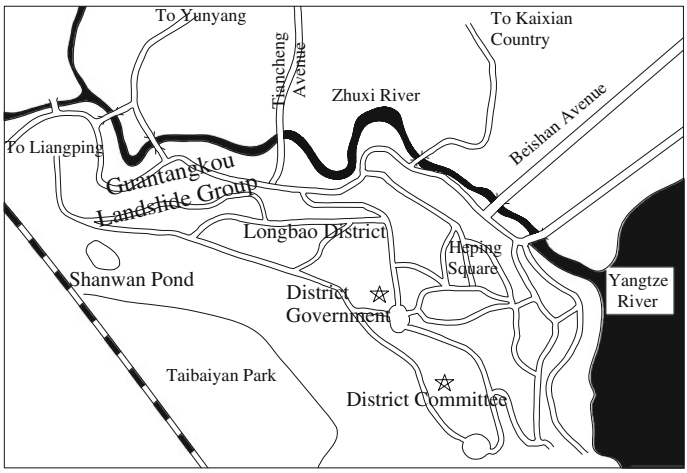

Fig. 8.5 Location of the Guantangkou landslide in Wanzhou

area is about 0.4 km^2 and total volume is about 1280 × 104 m^3. The whole sliding body is mainly composed of quaternary block clamp silty clay, silty clay, and gravel rock. The rock composition is mainly sandstone and mudstone. According to the trial pit water penetration test, silty clay proves to be a good waterproof performance. Groundwater of slippery body is mainly recharged by atmospheric precipitation and surface water, and flow path is short, discharging at low point of the terrain. Thus, the groundwater occurrence condition is poor and inhomogeneity in the accumulated layer landslide.

(2) Selection of calculation scheme

The landslide of Guantangkou is located at mid-front of Taibai rock history sliding body, and it is still stable as a whole with some extent signs of deformation. The bottom edge deformation mainly occurred at shallow parts of the Guantangkou slope according to the survey. The II–II′ and V–V′ profiles are selected to be calculated combing with the analysis of landslide stability. The methods of Fillennius, Bishop, Janbu, and transfer coefficient are selected to evaluate the stability, because the landslide zone shows circular arc and break line shapes. Landslide thrust is obtained using transfer coefficient method and checked using other methods.

(3) Selection of parameters of soil physical and mechanical properties in sliding zone

Some parameters of soil physical and mechanical properties at selected profiles in sliding zone are shown in Table 8.2. These parameters are obtained through the exploration of the hole and shaft in soil sample in indoor test and in situ shear test.

Natural weight of side body is 20.3 kN/m^3, and saturated weight is 20.6 kN/m^3. Values of shear strength parameters are determined after comprehensive judgements and inverse analysis listed in Table 8.3.

Table 8.2 Physical and mechanical parameters of the Guantangkou landslide

Natural state				Saturated state			
Peak		Salvage value		Peak		Salvage value	
c (kPa)	φ (°)	c (kPa)	φ (°)	c (kPa)	φ (°)	c (kPa)	φ (°)
38.14	17.17	29.93	13.49	27.46	13.82	19.86	9.59

Table 8.3 Stability analysis and calculation parameter selection

	Natural state		Saturated state	
	c (kPa)	φ (°)	c (kPa)	φ (°)
The sliding zone	30	15	21	13.5
Trailing shallow edge	27	12.9	20	12.5

(4) Calculation model and load combination of landslide.

1. Calculation model

Form line of sliding slope and sliding slice are both simplified into broken lines when calculating by Calslope procedure, where slide unit width is 1 m, which could be applied into two-dimensional calculation.

2. Load combination

a. Self-weight: there is no concentrated load but self-weight in sliding body.
b. Acting force of groundwater
The geological exploration indicated that seepage field was formed in landslide under the action of rainfall infiltration. So, buoyancy produced by pore water pressure on sliding zone should be taken into account, as well as the influence of rainstorm on landslide stability.
c. Water table of the Three Gorges Reservoir

Both storage table and reservoir regulation have various influences on the landslide stability after the completion of the Three Gorges Project. Therefore, the following two aspects should be taken into account when calculating, that is, ① the effect of normal storage table (i.e., 175 m) on landslide stability; and ② calculation of landslide stability when water table drops (i.e., from 175 m down to 145 m).

3. Working condition combination

a. Working condition 1: dead weight and heavy rain K_s = 1.25 (overall), K_s = 1.20 (trailing shallow edge).
b. Working condition 2: dead weight and water table at 175 m, K_s = 1.15.
c. Working condition 3: dead weight, water table from 175 to 145 m and rainstorm K_s = 1.15.

Working conditions of each computation section are shown in Figs. 8.6 and 8.7.

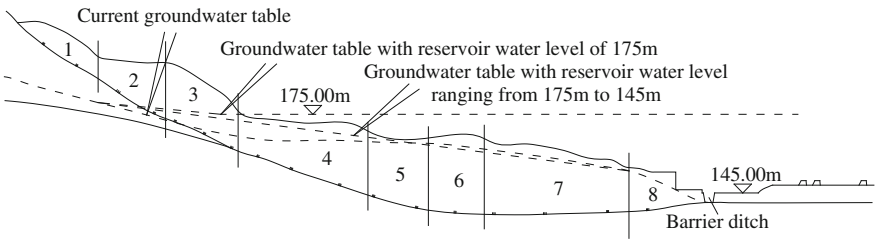

Fig. 8.6 Sketch map of landslide stability calculation at II–II′ profile of Guantangkou slope, Wanzhou

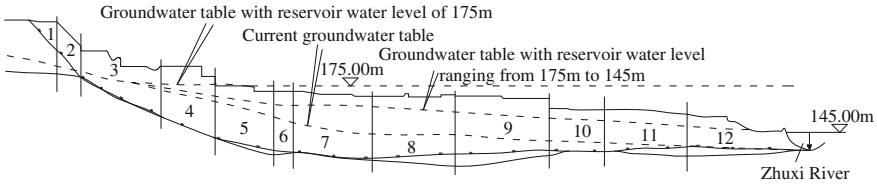

Fig. 8.7 Sketch map of landslide stability calculation at V–V′ profile of Guantangkou, Wanzhou

2. Data for calculation

Quantitative analysis results on landslide stability of Guantangkou landslide are listed in Tables 8.4 and 8.5.

3. Results of stability analysis and calculation

Calculation results of stability analysis of Guantangkou landslide under the working conditions of 1–3 are shown in Tables 8.6 and 8.7.

4. Analysis on calculation of landslide thrust.

It is essential to divide slide body into slices when calculating thrust (Figs. 8.6 and 8.7). Residual sliding force is calculated under three conditions based on basic loads, self-weight, and aquiferous groups. The residual slide force is zero in the cases of basic loads. In order to make a trend analysis and comparison, though the residual sliding force is determined by calculated values in theory, the value is considered as zero in real designing. In this book, the slices method is adopted.

(1) Calculation results of landslide thrust at V–V′ profile

The landslide thrust (kN) is shown in Table 8.8 when water table reaches 175 m and security coefficient equals to 1.15. Landslide thrust under the following two conditions are, respectively, calculated with seismic acceleration of 0, 0.05g and 0.1g: saturated slide zone and no groundwater table; mere hydrostatic pressure with groundwater table.

Table 8.9 indicates the value of landslide thrust with security coefficient of 1.15 when water table drops from 175 to 145 m. The working condition of considering groundwater table and seepage pressure is introduced after comparing with Table 8.8.

Calculation results listed in Table 8.9 shows that as for No. 8 slice, landslide thrust equals to zero when seismic acceleration equals to zero under saturated sliding zone condition. Landslide thrust equals to 1334 kN under only hydrostatic pressure condition. Landslide thrust equals to 3138 kN under seapage pressure condition. Similarly, landslide thrust equals to 8936 kN when seismic acceleration equals to 0.1g under saturated sliding zone condition. Landslide thrust equals to 24,237 kN under only hydrostatic pressure condition. Landslide thrust equals to 26,041 kN under seepage pressure condition. These results show an increasing tendency with the order increase of the above-mentioned conditons.

Table 8.4 Calculation of landslide stability at II–II′ profile of Guantangkou landslide in Wanzhou

Profile number	Soil slice	Boundary	X Coordinate (m)	Slope crest (m)	Slip band (m)	Water table (m)			Natural state		Saturated state		Imposed load (kN)
						Cond. 1	Cond. 2	Cond. 3	c (kPa)	φ (°)	c (kPa)	φ (°)	
II–II′		X1	5	213	213	213	213	213	27	12.9	20	12.5	0
	1	X2	37.44	200.05	190.02	190.02	188.91	180.98	27	12.9	20	12.5	0
	2	X3	64.79	196.68	174.29	174.36	177.99	177	30	15	21	13.5	0
	3	X4	93	176.9	161.41	166.91	175.4	173.07	30	15	21	13.5	0
	4	X5	144.93	167.99	143.2	165.17	167.99	166.14	30	15	21	13.5	0
	5	X6	168.55	166.85	137.26	164.08	166.85	164.42	30	15	21	13.5	0
	6	X7	191.05	166.2	135.22	161.88	166.2	162.31	30	15	21	13.5	0
	7	X8	247.6	154.06	136.37	153	154.06	153.11	30	15	21	13.5	0
	8	X9	279.02	145.9	140.4	140.8	145.9	140.4	30	15	21	13.5	0

Table 8.5 Calculation of landslide stability at V–V′ profile of Guantangkou Landslide in Wanzhou

Profile number	Soil slice	Boundary	X Coordinate (m)	Slope crest (m)	Slip band (m)	Water table (m)			Natural state		Saturated state		Imposed load (kN)
						Cond. 1	Cond. 2	Cond. 3	c (kPa)	φ (°)	c (kPa)	φ (°)	
V-V′		X1	17.49	218.79	218.79	218.79	215	218.79					
	1	X2	37.16	216.73	198.08	198.08	198.08	198.08	27	12.9	20	12.5	0
	2	X3	55.25	198	183.44	183.44	183.44	183.44	27	12.9	20	12.5	0
	3	X4	111.59	188.13	155.96	173.25	176.95	174.31	27	12.9	20	12.5	0
	4	X5	151	181.3	142.56	165.9	175	169.1	30	15	21	13.5	0
	5	X6	192.28	171.86	133.97	155.7	171.86	164.54	30	15	21	13.5	0
	6	X7	206.28	171.78	132.65	152.25	171.78	163.29	30	15	21	13.5	0
	7	X8	263.67	168.51	128.5	144.38	168.51	161.85	30	15	21	13.5	0
	8	X9	323.21	168.93	131.09	143.22	168.93	158.68	30	15	21	13.5	0
	9	X10	390.61	166	133.49	140.02	166	154.88	30	15	21	13.5	0
	10	X11	430.6	159.8	133.3	138.77	159.8	152.51	30	15	21	13.5	0
	11	X12	489.27	156.27	135.59	136.59	156.27	149.02	30	15	21	13.5	0
	12	X13	580	133.5	133.5	133.5	133.5	133.5	30	15	21	13.5	0

Table 8.6 Calculation results of landslide stability coefficient when water tables dropped from 175 to 145 m at II–II′ profile

Woking conditions	$a = 0g$				$a = 0.05g$			
	Fillennius	Bishop	Janbu	Transfer coefficient	Fillennius	Bishop	Janbu	Transfer coefficient
Saturated slide band	1.444	1.4961	1.4844	1.55	1.1506	1.1825	1.1824	1.22
Hydrostatic pressure	1.0102	1.0581	1.046	1.09	0.8016	0.8305	0.8267	0.85
Hydrostatic and osmotic pressure	0.9674	1.0142	1.0035	1.05	0.7642	0.7916	0.7886	0.82

Table 8.7 Calculation results of landslide stability coefficient when water tables drops from 175 to 145 m at V–V′ profile

Woking conditions	$a = 0g$				$a = 0.05g$			
	Fillennius	Bishop	Janbu	Transfer coefficient	Fillennius	Bishop	Janbu	Transfer coefficient
Saturated slide band	2.5495	2.6311	2.5035	2.83	1.7379	1.7842	1.751	1.86
Hydrostatic pressure	1.8267	1.905	1.8328	2.03	1.2418	1.2849	1.2689	1.33
Hydrostatic and seepage pressure	1.7567	1.8327	1.766	1.96	1.1968	1.2388	1.2247	1.29

Table 8.8 Landslide thrust with normal water table of 175 m at V–V′ profile (unit:kN)

Saturated slide band			Hydrostatic pressure		
$a = 0g$	$a = 0.05g$	$a = 0.1g$	$a = 0g$	$a = 0.05g$	$a = 0.1g$
2090	2276	2462	2180	2367	2554
5072	5582	6092	5179	5689	6199
11438	13504	15570	13069	15146	17223
14381	18104	21826	18523	22274	26025
12940	18504	24068	20414	26031	31649
10715	16767	22819	19217	25330	31443
1878	10712	19547	15678	24613	33548
0	0	8936	4942	16420	27898
0	0	0	0	9265	23684
0	0	0	0	6827	22842
0	0	0	0	2030	19565
0	0	0	0	0	18179

Table 8.9 Calculation results of landslide thrust when water tables drops from 175 to 145 m at V–V′ profile (unit:kN)

Saturated slide band			Hydrostatic pressure			Seepage pressure		
$a = 0g$	$a = 0.05g$	a = 0.1g	$a = 0g$	$a = 0.05g$	$a = 0.1g$	$a = 0g$	$a = 0.05g$	$a = 0.1g$
2090	2276	2462	2090	2276	2462	2090	2276	2462
5072	5582	6092	5092	5602	6111	5112	5622	6132
11438	13504	15570	12704	14879	16954	13408	15484	17559
14381	18104	21826	17857	21603	25350	19006	22753	26499
12940	18504	24068	19117	24725	30334	20687	26295	31904
10715	16767	22819	17701	23804	29906	19314	25417	31519
1878	10712	19547	13148	22064	30981	14888	23804	32721
0	0	8936	1334	12786	24237	3138	14589	26041
0	0	0	0	3843	18324	0	5874	20255
0	0	0	0	594	16563	0	2628	18597
0	0	0	0	0	12356	0	0	14438
0	0	0	0	0	10096	0	0	12278

However, calculation results in Tables 8.8 and 8.9 show that under the same security coefficient (K_s = 1.15), landslide thrust under water table of 175 m, in slice 8 for an example: a = 0, P = 0 (saturation), P = 4942 kN (hydrostatic pressure); a = 0.1g, P = 8936 kN (saturation), P = 27898 kN (hydrostatic pressure), the landslide thrust are higher than that of the water tables dropped from 175 to 145 m. It indicates that landslide stability does not always decrease when water table of the Three Gorges Reservoir drops from 175 to 145 m. The thin landslide with smooth sliding zone is helpful for landslide stability due to the decrease of sliding body underwater and small hydraulic grade, indicating that the decreasing rate of landslide buoyancy is higher than the increasing rate of seepage pressure.

(2) Calculation results of landslide thrust at II–II′ profile

Table 8.10 shows the landslide thrust when water table of the Three Gorges Reservoir equals to 175 m. Table 8.11 shows the landslide thrust when water table of the Three Gorges Reservoir drops from 175 to 145 m. The conclusion is the same as that at V–V′ profile.

5. Evaluation of landslide stability

1. The stability under current situation

Above stability analysis and calculation indicates that the landslide of Guantangkou is stable except the western parts, i.e., II–II′ profile under current self-weight and storm rain situation. In the process of calculation, the effect of hydrostatic pressure on slide is considered, however, accurately, the trailing edge cracks on the Shalong road is closed of emulsified asphalt and drainage ditches are built. A poor infiltration capacity of slide is found in the process of landslide investigation. stability coefficient at II–II′ profile is low due to hydrostatic pressure. The western part on Guantangkou landslide is unstable under self-weight and rainstorm conditions. It is possible that landslide will become unstable if drainage condition is poor when raining heavily.

Table 8.10 Landslide thrust with normal water table of 175 m at II–II′ profile (unit:kN)

Saturated slide band			Hydrostatic pressure		
a = 0g	a = 0.05g	a = 0.1g	a = 0g	a = 0.05g	a = 0.1g
882	1066	1251	882	1066	1251
3828	4531	5234	3910	4614	5317
6024	7360	8696	6723	8064	9405
8142	10741	13340	11287	13908	16529
8072	11406	14740	12686	16053	19420
5235	9251	13268	11229	15289	19349
0	1718	7281	5149	10777	16406
0	0	4265	2171	8060	13948

Table 8.11 Landslide thrust when water tables drops from 175 to 145 m at II–II′ profile (unit:kN)

Saturated slide band			Hydrostatic pressure			Seepage pressure		
$a = 0g$	$a = 0.05g$	$a = 0.1g$	$a = 0g$	$a = 0.05g$	$a = 0.1g$	$a = 0g$	$a = 0.05g$	$a = 0.1g$
882	1066	1251	882	1066	1251	882	1066	1251
3828	4531	5234	4029	4734	5438	4121	4825	5530
6024	7360	8696	6723	8064	9405	6985	8326	9667
8142	10741	13340	11021	13641	16260	11873	14492	17111
8072	11406	14740	12305	15669	19034	13327	16692	20057
5235	9251	13268	10700	14755	18811	11808	15863	19919
0	1718	7281	4319	9941	15564	5448	11070	16693
0	0	4265	1136	7016	12897	1849	7730	13611

2. Landslide stability under reservoir table and scheduling conditions of the Three Gorges Reservoir

The landslide stability of Guantangkou landslide proves to be the worst according to the above calculation when water table reaches 175 m. Front part of the Guantang landslide is the anti-sliding segment with smooth topography and water table is lower than 175 m resulting in a poor infiltration capacity. When water table drops from 175 to 145 m, negative influence of the increasing groundwater seepage pressure on landslide is weaker than positive influence of decreasing buoyancy on landslide. Therefore, landslide stability of Guantangkou increased comparing with that when water table is 175 m. The landslide condition is the worst under water table of 175 m and heavily rainfall conditions. Water table is 175 m, stability coefficient at II–II′ profile equals to 1.03, which indicated a unstable status. However, stability coefficient at V–V′ profile ranges from 1.5 to 1.6, showing a good global stability.

8.5.2 Groundwater of the Tunnel Project

Fissure water of bedrock is one of the most common groundwater in China. In engineering projects of tunnel, dam and other large underground constructions, the enrichment of bedrock fissure water directly pose a threat to the construction and operation management, rising a number of special engineering problems, such as landslide, roof caving, water gushing or inrush, and even the underground debris flow and tunnel deformation, etc. According to the statistics of the 415 tunnels of the Nan-Kun railway, landslides occurred in 15 %, and water burst occurred in 93.5 % of these tunnels. More than 60 collapses occurred in 11 faults of the GuanJiao tunnel during the construction of the Qinghai–Tibet railway. The short-term maximum fissure water discharge of the 9th fault was 38,000 t/d and 29 massive landslides occurred during the construction of the Dayaoshan tunnel. The reasons for collapses may be that, bedrock fissure water immersed and softened the structural plane, soft layer and the fracture zone, reducing its strength and taking away the fillings of the weak surfaces. The rock mass would disintegrate quickly, inducing or worsening the collapses. The occurrence of bedrock fissure water mainly depends on the bedrock type (Table 8.12). However, due to uneven burial distribution of bedrock fissure water, and complexity of its occurrence and transport, there was little hydrogeological research for bedrock area, which should be taken into consideration seriously. As engineering example, the bedrock fissure water of new Qidaoliang tunnel area was introduced.

Table 8.12 Structure types of fractured rock

Structure types	Fissure surface	Integrity coefficient	Permeability	Quantitative model
Massive structure	Few fractures, microcracks	>0.9	Hardly impermeable	Continuous medium
Blocky structure	Generally developed joints	0.6–0.8	Poor permeability	Noncontinuous medium
Stratified structure	Relatively developed fractures	0.3–0.6	Obvious anisotropy permeability	Noncontinuous medium
Cataclastic structure	Developed fractures	0.1–0.3	High permeability	Noncontinuous medium
Unconsolidated structure	Developed fractures	<0.1	Strong permeability	Seem-continuous Medium

8.5.2.1 Geologic Features of Bedrock Fissure Water in New Qidaoliang Tunnel Area

Qidaoliang is the watershed of Qilihe district of Lanzhou and Lintao county of the Dingxi region, and belongs to the temperate zone with semiarid climate. North slope of the area is dankness, but the southern slope is dry and rainless. Annual precipitation is 500 mm and the evaporation is 1500 mm. Tunnel site belongs to low mountainous area. Topography steep, exposed bedrock, erosional and structural fissures are developed at north part of the watershed. It is advantageous for precipitation to infiltrate bedrock and form the fissure water. The topography is gradual at south of the watershed, and the overlying eolian loess that contains no water is 3–15 m. Due to the presence of mudstone at the bottom of the loss, there may be some fissure and pore water in weathered zone of the mudstone and overlying eolian loss. If fractures are developed at the bottom of the loess, the bedrock fissure water would formed by the infiltrated loess water. Bedrock fissure water in the area is mainly distributed in sandstone and conglomerate of the Hekou group. Due to the various rock structure character and size, and terrains of the area, the groundwater is uneven distribution with various water abundances.

Bedrock fissure water of the tunnel site is mainly recharged by precipitation, which seeps into ground through the small thickness of quaternary overburden and bedrock weathering zone. Then the water flows along the bedrock fissures forming the fracture phreatic water, and may be accumulated at the local parts of tectonic fracture zone. The bedrock fissure water finally discharges at depression springs of the slope. The small scale of confined water may also be formed at some local regions with certain constructs, terrains, impermeable and permeable layers and attitude of rock formations. Dynamic of groundwater table was affected by climate, hydrogeological conditions. The depth of water table increased in dry seasons, resulting in decreased water discharge. The situation was opposite in wet seasons with decreased depth of water table and increased water discharge.

8.5.2.2 The Partition of Bedrock Fissure Water, According to the Seepage Characteristics

Surrounding rock of New Qidaoliang tunnel was characterized as the dual pore-fracture medium, and fissure water was the basic groundwater type. Thus the distribution of groundwater is uneven, with various water abundances of the tunnel surrounding rock.

1. Southern entrance—F4 fault

(1) Engineering geological conditions

The lithology of this section was mainly characterized as weathering conglomerate, conglomerate, silicide crystalline limestone, phyllite, and F4 fault. Weathering conglomerate and conglomerate were flat and integrity, with not very developed fault and joint. Limestone and phyllite section have the steeply dipping occurrence and folds along the tendency. Limestone is hard and relatively complete with developed fissures. Phyllite has the thin plate structure which is softness and poor integrity. F4 fault, the thrust fault with steep dip angle, is the regional major fault with the trend of 315° and dip angle of 74°. The width of the fault and the affected zone, filled with fault gouge, breccia, rock fragments and phyllite, etc., is about 120 m.

2. Seepage analysis

Entrance section of the tunnel is in vadose zone, recharged by infiltration of the precipitation and surface water. Thus, it is wet in the entrance section of the tunnel because of the fissure water infiltration in rainy season, and is desiccation in the dry season with not a large number of water burst in generally. Due to no incision of large geological structural plane, Limestone is only with the joint and fissure water which are not too much. Phyllite which is dry and has no water acts as an aquiclude. Only crack ooze water and moist occur in the partial phyllite section. F4 fault and the influence zone with the characteristics of rich water, full water and water resistance, mainly filled with the fault mud, form the aquitard and divide the hanging wall and footwall into two different hydrogeological units. Hanging wall is the medium-thickness layered rock of the limestone with embed phyllite or interbed limestone and phyllite, the resisted bedrock fissure water is enriched at the hanging wall. Lithology of the footwall is sandstone embed mudstone or interbed limestone and phyllite. Due to the control of lithology and tectonic interface, the enrichment zone of interval structure crevice water was developed.

According to the observation statistics of water discharge after the tunnel excavation, the water burst and seepage phenomena were only in the section of XK21 + 045–XK20 + 825. Vault, left and right side of the tunnel wall occurred different scales of the water burst and seepage, but most water burst points distributed at the right tunnel wall. The lithology of this segment is crystalline limestone characterized as the hard brittle rock with developed fissures, forming the

Table 8.13 Entrance—statistical water discharge of F4 fault in tunnel

Mileage	Lithology	Rock structural types	Structural planes	Rich-water area	Measured water discharge (t/d)		Dynamic	Predicted water discharge (t/d)	Deviation (t/d)
					Maximum (location)	Average			
XK21 +440–+270	Weathering conglomerate, conglomerate and fault fracture zone (F5)	Layered and unconsolidated structure	Developed fractures	Vadose zone with basically no water	No water	No water	Unstable and obviously affected by precipitation	No water	
XK21 +270–XK20 +800	Siliceous limestone with interbed phyllite	Block-layer structure	Developed fractures	Abundant fissure water	48.22 (XK20 + 911, Right Wall)	42.50/300 m	Stable and unconspicuous affected by precipitation	50/300 m	−7.5/300 m
XK20 +800–+690	F4 fault	Unconsolidated structure	Developed fractures	Squeezing fissures with basically no water	1.227 (XK20 + 691, Right Wall)	0.41/110 m	Stable and unconspicuous affected by precipitation		

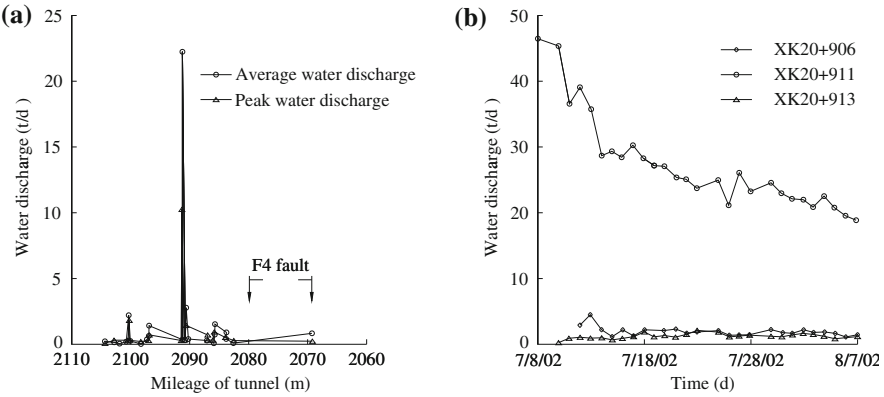

Fig. 8.8 Tunnel entrance water discharge curves F4 fault. **a** water discharge variation on mileage. **b** water discharge variation time

bedrock fissure water. Comparison of the designed and forecast and actual observation water discharge contrast was shown in Table 8.13 and Fig. 8.8.

2. F4 fault—F3 fault

1. Engineering geological conditions

This section is located in the Shuichi river valley, the southern and northern parts of which are the F3 and F4 faults zone. The basic bedrock lithology is sandstone interbed mudstone which is medium thickness-thick layer with rock breakage, developed fractures and local small fold with an asymmetric syncline. F3 fault is a normal fault with steep dip angle of 60°, strike of NW to SE and tendency of SW. The stratums of both hanging wall and footwall of the fault were Hekou group of lower cretaceous. The fault was filled with broken sandstone and mudstone with developed fissures and poor integrity.

2. Seepage analysis

Fracture development is closely controlled by lithology and fold structure. The characteristics of fissures development are obviously different in sandstone and mudstone, and fissures in sandstone are interpenetration with each other. Due to the strong rigidity, the sandstone in general with tension fractures which have high connectivity, become a relative aquifer. The mudstone is a relative aquitard due to its soft plastic character with fine and close of joints and poor water conductivity. The fracture water of sand and mudstone is relatively in layers, so that the interlayer fissure water is under pressure. Because of the fissure water in layers, the amount of fissure water is decreased with depth increasing. Sandstone aquifers are separated by mudstone layer, resulting in no hydraulic connections and transfluence of two aquifers. F3 fault was a small fault with the hanging wall of sandstone interbeded mudstone layer. The groundwater was recharged rainfall and surface water infiltration. The main recharge source is Shuidi river that infiltrates under gravity

Table 8.14 Statistical water discharge of F4–F3 fault section

Mileage	Lithology	Rock Structural types	Structural planes	Rich water area	Measured water discharge (t/d)		Dynamic	Predicted water discharge (t/d)	Deviation (t/d)
					Maximum (location)	Average			
XK20 +690–+370	Sandstone with interbed mudstone	Layered structure	Developed fractures	Abundant fissure water	24.19 (XK20 +536, Right wall)	122.47/300 m	Unstable and obviously affected by precipitation	938/500 m	−440.33/300 m
XK20 +370–+320		Unconsolidated structure	Developed fractures	Abundant fissure water	4.46 (XK20 +363, Vault)	19.33/50 m	Stable and unconspicuous affected by precipitation		

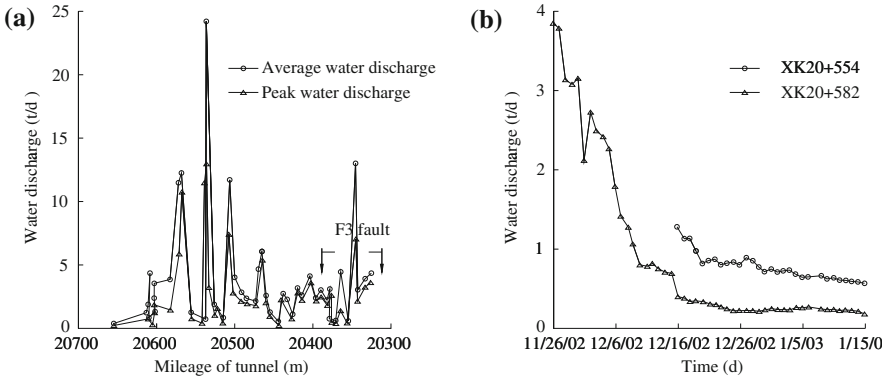

Fig. 8.9 Water discharge curves of F4 fault—F3 fault section. **a** Water discharge variation on mileage. **b** Water discharge variation time

through the surface fissures and weathered zone. Thus hanging wall of F3 fault had the rich water. Water containing and strong transport properties of the F3 fault, not only resulted in the drainage of fissure water in sand and mudstone layers, but also resulted in the strongly discharge of fissure water in the weathered zone with sharply declined water table.

According to the excavation of tunnel water discharge after observation statistics, the design water discharge forecast and actual observation contrast are shown in Table 8.14 and Fig. 8.9.

8.5.2.3 Conclusions

The fissure water seepage of bedrock brings great influence on construction of large underground engineering. Understanding its seepage features has realistic meaning. However, the study and governance of bedrock fissure water are very difficult due to the complex groundwater seepage in fractured rock. According the process of tunnel excavation of new Qidaoliang tunnel, the analysis results of water seepage observation of the tunnel indicated the following conclusions:

1. Due to random distribution and anisotropy connectivity of the vast fractures in rock mass, the occurrence and status of bedrock fissure water are various, resulting in the heterogeneity of seepage.
2. Groundwater flow in fractured rock mass is closely related to the fracture occurrence, and anisotropy of the fissures caused the anisotropy of fissure water seepage.
3. Most water burst points distributed at right side wall of the downlink of the New Qidaoliang tunnel, suggesting that the connectedness of the fissures in rock mass is strong and river recharge has a certain influence on the tunnel water discharge.

4. During the excavation of Qidaoliang tunnel, when water discharge was mainly from storage resource, initial water discharge was very large characterized by sudden flood water. However, the water discharge decreased quickly with the passage of time, rarely has the stable status (see dynamic curves of water discharge of XK20 + 911 in Fig. 8.8 and XK20 + 582 in Fig. 8.9). When water discharge was mainly from the recharge resource of surrounding rock, the water discharge tended to remain a relatively stable flow (see dynamic curves of water discharge of XK20 + 906 and XK20 + 913 in Fig. 8.8, and XK20 + 554 in Fig. 8.9).

8.6 Exercises

1. How to categorize the bedrock groundwater according to the hydraulics and medium types? Is it perfect?
2. What are the burial characteristics of bedrock fissure water? What are the laws involved in groundwater occurrence and migration?
3. The fracture-pore dual-medium model is divided into two types; what are they and the assumptions in them?
4. Review literatures and understand the new progress of groundwater seepage models of fractured rock mass.
5. How many numerical simulation softwares can be used to depict the bedrock fissure water? What is the process?
6. List the engineering examples associated with bedrock fissure water, and briefly expounds the influences of bedrock groundwater.